RESEARCH ARTICLE

Interactions of Hydrogen Atoms with Acceptor–Dioxygen Complexes in Czochralski-Grown Silicon

Tarek O. Abdul Fattah,* Vladimir P. Markevich, Joyce Ann T. De Guzman, José Coutinho, Stanislau B. Lastovskii, Ian D. Hawkins, Iain F. Crowe, Matthew P. Halsall, and Anthony R. Peaker

It is debated in the silicon PV community whether or not the presence of hydrogen is essential for the permanent suppression ("regeneration") of the recombination activity of the boron–oxygen (BO) defect, which is responsible for light-induced degradation (LID) of solar cells produced from B-doped oxygen-rich silicon. The BO-LID defect has been identified as a B_sO_2 complex which has negative-U properties. This study focuses on the interactions of hydrogen with the B_sO_2 defect to elucidate the BO-LID regeneration mechanism. With the use of junction spectroscopy techniques, the changes in concentration of the B_sO_2 donor state in diodes which are fabricated on Czochralski-grown (Cz) B-doped Si and subjected to hydrogenation and subsequent heat treatments have been monitored. It is found that annealing of the hydrogenated Cz-Si:B diodes in the temperature range 398–448 K under the application of reverse bias (RBA) results in nearly total disappearance of the B_sO_2 defect. It is argued that electrically neutral B_sO_2–H complexes have been formed upon the RBA treatments. According to ab initio calculations, the binding energy of H^+ to $B_sO_2^-$ exceeds that of H^+ to B_s^- by at least 0.1 eV, and the resulting B_sO_2–H complexes are electrically inactive.

1. Introduction

Solar cells made from crystalline silicon doped with boron and containing significant amounts of oxygen suffer from the degradation of minority carrier lifetime and conversion efficiency upon the early stages of operation under illumination, commonly called "light-induced degradation (LID)." The detrimental effect of this degradation mechanism on the performance of the Si solar cells (solar conversion efficiency drops up to 10% relative or 2% absolute over time) has driven intense research efforts to eliminate the impact of recombination activity associated with the formation of the boron–oxygen (BO) defect, particularly in Czochralski-grown boron-doped silicon material (Cz-Si:B). It is well established that the minority carrier lifetime and conversion efficiency degradation process is associated with a complex of one boron atom and two oxygen atoms.[1,2]

Compelling evidence was recently presented that the complex, which consists of a substitutional boron atom and the oxygen dimer (B_sO_2 defect), is a defect with negative-U properties.[3–5] The B_sO_2 defect undergoes a transformation from the deep donor state, which is recombination inactive, into a shallow acceptor state with enhanced recombination activity upon prolonged minority carrier injection.[3,4] It has been argued that the B_sO_2 defect in the shallow acceptor state is responsible for BO-LID.[3,4] The interactions between other substitutional acceptor atoms, A_s (A_s being either Ga, Al, or In), and the interstitial oxygen dimer in p-type Cz-grown silicon have been also reported resulting in the formation of A_sO_2 defects.[5] All members of the family of defects formed due to the interactions of group III elements with the oxygen dimer in silicon exhibit negative-U properties and are deep donors in the ground state in p-type Si.

T. O. Abdul Fattah, V. P. Markevich, I. D. Hawkins, I. F. Crowe,
M. P. Halsall, A. R. Peaker
Photon Science Institute and Department of Electrical and Electronic Engineering
The University of Manchester
Manchester M13 9PL, UK
E-mail: tarek.abdulfattah@postgrad.manchester.ac.uk

The ORCID identification number(s) for the author(s) of this article can be found under https://doi.org/10.1002/pssa.202200176.

J. A. T. De Guzman
Philippine Council for Industry, Energy, and Emerging Technology Research and Development
Department of Science and Technology (DOST)
Taguig City, Metro Manila 1631, Philippines

J. Coutinho
I3N and Department of Physics
University of Aveiro
3810-193 Aveiro, Portugal

S. B. Lastovskii
Scientific-Practical Materials Research Center
NAS of Belarus
Minsk 220072, Belarus

Upon illumination, the BO defect, which gives rise to LID, is converted from an initial state often named the "annealed state" to a degraded state which is metastable and can be transformed back to the annealed state (unstable recovery) by dark annealing at 200 °C for several minutes.[1,2] Importantly, the degraded state can be converted into a stabilized state,[2,6,7] also called the "regenerated state"[2] via illuminated annealing at slightly elevated temperatures.[6–9] This state is characterized by the stable recovery of the minority carrier lifetime back to predegradation values via the regeneration treatment. Unfortunately, the destabilization, which is the reverse reaction from the regenerated state to the annealed state, can still occur via dark annealing at 200 °C for about 100 min.

The hypothesis that hydrogen plays a key role in the regeneration mechanism of the BO-LID defect has been proposed by many research groups after being reported in 2009.[9] It has been shown that the presence of mobile atomic hydrogen in the silicon bulk is necessary for regeneration and that no or only extremely slow regeneration is possible without hydrogen.[10–14] The hydrogen is usually introduced into the bulk regions of Si solar cells via diffusion from hydrogen-rich silicon nitride layers during high-temperature firing, which is necessary for formation of metal contacts for the cells. The effective BO-LID regeneration requires an appropriate amount of hydrogen to be present in the bulk of the Si material. From the analysis of BO-LID regeneration kinetics, the following influencing factors have been determined: 1) the presence of a hydrogen source to supply enough amount of hydrogen for complete regeneration (e.g., H-rich silicon nitride layers);[11–14] 2) firing temperature, which affects the introduction of hydrogen into the bulk;[11,13,14] and 3) cooling rate after firing.[11] The properties of the nitride layers, i.e., their thickness, SiH_4 and NH_3 gas flow ratio, and layer composition, were found to affect the amount of hydrogen diffused into the bulk upon firing. This is in agreement with the finding that the different structures of surface coating (SiO_2/SiN_x, Al_2O_3/SiN_x) have no influence on the BO-LID regeneration rate as long as they introduce the same amount of hydrogen into the bulk.[13] The introduction of hydrogen from the passivation layers can also be enhanced by the firing conditions. It has been found that the regeneration rate is accelerated by a higher firing temperature and a longer duration at this temperature (known as the peak width).[11] Further, a fast cooling down after firing is needed for effective regeneration to occur. It has been argued that the fast cooling down to 500 °C is necessary to stop the net effusion of hydrogen from the silicon bulk, which decreases the hydrogen content available for the passivation of the BO defect.[13,15]

It has been suggested that oxygen also plays a role in the BO deactivation process.[15] The evidence presented for this is that the kinetics of deactivation reaction of the BO defect is inversely affected by the presence of interstitial oxygen and/or oxygen clusters (thermal donors), which result in a lower deactivation rate and smaller value of lifetime after complete deactivation.[15] Moreover, it has been argued that hydrogen is responsible for passivation of background unknown defects, which affect the lifetime, and it is not required for the BO-LID regeneration.[14] In a more recent study, it was proposed that the overall regeneration of the BO defects is composed of two different mechanisms.[16] It was found that while hydrogen plays no role in the BO-related lifetime degradation mechanism, it is only involved in one of the regeneration mechanisms while the other can occur without hydrogen.[16]

A possible source of hydrogen within the Si, important for regeneration, is the B–H pairs. It was proposed that during regeneration conditions, splitting of B–H pairs can occur (under carrier injection) which increases the concentration of bulk hydrogen available to contribute to regeneration.[17] Any thermal conditions (e.g., slower cooling rate after high-temperature firing), which result in the formation of more stable hydrogen complexes (compared to B–H) such as H_2 molecules, can have a detrimental effect on the kinetics of the BO regeneration. It was proposed that the passivation of BO defects by neutral hydrogen atoms, H^0, is responsible for the regeneration.[17]

The regeneration reaction can be accelerated by high-temperature/high-injection conditions. It has been argued that these conditions are needed to enhance the defect degradation rate, rather than the defect passivation rate, subsequently improving the effectiveness of regeneration.[18–20] With the aim of using the regeneration treatments commercially, it has been shown that regeneration of hydrogenated samples can be completed in less than 10 s at 200–230 °C under 2.7 suns illumination.[12,18,20] The BO-LID regeneration can be further accelerated (completed in 0.5 s) via a laser illumination treatment, which provides simultaneous heat and carrier injection.[13]

In this work, we present experimental results which support the arguments that the regeneration of the BO defect is not possible without hydrogen. Further, we report experimental evidence of the formation of electrically inert B_sO_2–H complexes due to the interaction of hydrogen atoms with the B_sO_2 defect. We use capacitance–voltage (C–V) measurements to monitor the changes in the uncompensated ionized shallow acceptor profiles $N_A^-(W)$, which can be correlated with the movement of hydrogen in the samples upon different heat treatments. Conventional deep-level transient spectroscopy (DLTS) and high-resolution Laplace DLTS measurements were carried out on hydrogen-free diodes and on diodes hydrogenated either via wet chemical etching or via treatments in remote H plasma at room temperature. Measurements were carried out before and after reverse bias annealing (RBA) treatments of the hydrogenated samples at about 150 °C, which resulted in 1) the transformation of the B_sO_2 defect into the shallow acceptor state; 2) the separation of H atoms from the B_s–H complexes which were formed upon hydrogenation; and 3) the interaction of H^+ atoms with the $B_sO_2^-$ defects. According to ab initio calculations, the binding energy of H^+ to $B_sO_2^-$ exceeds that of H^+ to B_s^- by at least 0.1 eV, and the resulting B_sO_2–H complexes are electrically inactive. The obtained results are further discussed in the context of the regeneration of the recombination active BO defects. Some preliminary results on the interactions of hydrogen with Al_sO_2 and Ga_sO_2 complexes are also reported.

2. Experimental Results

2.1. Effect of Regeneration-Like Treatments on the Concentration of the B_sO_2 Defect in Cz-Si:B Samples with No Hydrogen

The n^+–p diodes used in this study have been fabricated with no significant amount of hydrogen introduced into the base regions during processing. The goal of this part of our work is to

investigate the effects of regeneration-like treatments (heat treatments in the range of 403–473 K with simultaneous minority carrier injection induced by forward current flow) on the changes in concentration of the B_sO_2 defects in the samples with negligible concentrations of hydrogen. In the conventional DLTS spectra recorded on all n^+−p diodes studied in this work, a hole-emission related peak with its maximum at about 390 K has been detected. This peak is assigned to hole emission from the donor state of the B_sO_2 complex, which is a precursor of the recombination active BO-LID defect (annealed state of the BO defect).[3,4] The details of the electronic structure of the B_sO_2 defect, parameters of the carrier emission and capture processes for its different configurations, peculiarities of its observation by junction spectroscopy techniques, and changes in the DLTS spectra induced by minority carrier injections and dark annealing treatments at different temperatures have been reported earlier in refs. [3,4]. In this work, the changes in the concentration of the B_sO_2 donor state have been monitored with the use of high-resolution DLTS measurements upon minority carrier injection (MCI) treatments with a current density $J_{FB} = 1.5$ A cm^{-2} at 350 and 423 K and upon dark annealing at 473 K after the carrier-injection treatments. The treatment at 350 K corresponds to a BO-related carrier-induced degradation regime and the treatment at 423 K to a BO-LID regeneration regime. **Figure 1** compares the evolution of the B_sO_2 donor state concentration upon carrier-injection treatments at 350 and 423 K.

The BO degradation mechanism is activated by minority carrier injection at 350 K and has been shown to be related to the transformation of the B_sO_2 defect from the deep donor to the shallow acceptor state.[3,4] This transformation is shown in Figure 1 by the exponential decay of the B_sO_2 donor state concentration upon continuous injection of minority carriers. The complete recovery of the defect concentration after dark annealing at 473 K for 10 min is another well-established feature of the BO-LID related processes. Further, the regeneration-like treatment, i.e., injection of minority carriers at slightly elevated temperature (423 K in this case),[7,20,21] resulted in a similar but

faster decrease in the concentration of the B_sO_2 donor state. Importantly, upon short time dark annealing at 473 K, a nearly complete recovery of the B_sO_2 donor state has been observed in the sample subjected to the regeneration treatment. This indicates that this treatment has not resulted in the true regeneration, i.e., the transformation of the B_sO_2 defect into the stable regenerated state (if the regenerated state is formed, no recovery of the B_sO_2 defect occurs after short time annealing at 473 K). It should be mentioned that the regeneration treatment in this case has been started when the B_sO_2 defect was in the annealed state. According to the literature results, the regeneration process occurs when the BO-LID defect is in the degraded state.[22]

To study the effect of the initial state of the B_sO_2 defect on the results of the regeneration treatments, further DLTS and high-resolution Laplace DLTS measurements have been carried out on n^+−p diodes from 10 Ω cm Cz-Si:B material. We have detected a similar hole emission-related peak with its maximum at 390 K in the conventional DLTS spectra of these diodes. The magnitude of the detected peak is slightly lower than that in the n^+−p diodes with a 3 Ω cm base that is expectable due to the lower boron concentration. The changes in concentration of the B_sO_2 donor state versus the minority carrier injection time at 423 K are shown in **Figure 2**, left. The effects of subsequent different injection/dark annealing treatments on the concentration of the B_sO_2 donor state are also presented in colored-filled part of Figure 2.

Upon minority carrier injection at 423 K, the concentration of the B_sO_2 donor state decays exponentially with time down to a saturation value after which no further decrease is attained upon longer forward bias injection. This can be explained by the competition between the degradation and annealing reactions at this temperature.[22] The annealing reaction results in the recovery of the concentration of the B_sO_2 donor state, while degradation reaction leads to the disappearance of this state. As the degradation reaction is slightly faster than the annealing reaction at 423 K, the resultant saturation value of the B_sO_2 donor state concentration in this case is fixed at about 3.5×10^{12} cm^{-3}. The
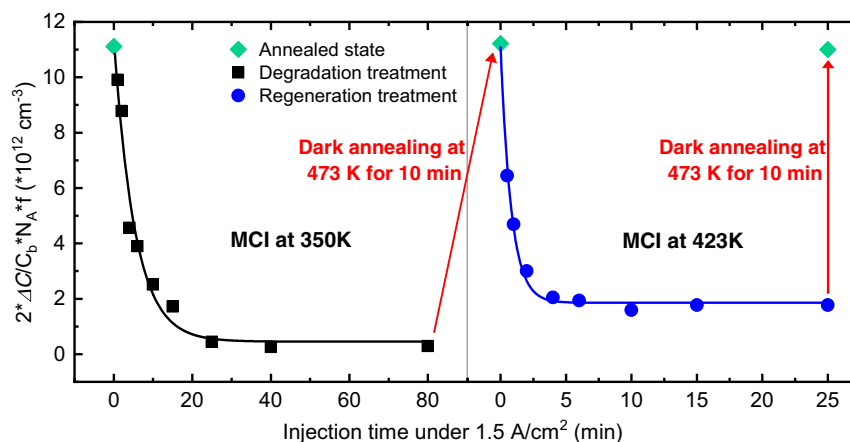

Figure 1. Changes in the concentration of the B_sO_2 donor state (precursor of the degraded state) upon degradation (left) and regeneration (right) treatments in 3 Ω cm boron-doped n^+−p diode. The degradation treatment was carried out at 350 K with the MCI induced by forward current with density $J_{FB} = 1.5$ A cm^{-2} and the regeneration treatment was carried out at 423 K with the same current density. After the degradation and regeneration treatments, the sample was annealed in the dark at 473 K for 10 min. Measurements of the concentration of the B_sO_2 donor state were carried out at 350 K with the use of Laplace DLTS technique for all data points. Solid lines are fittings of the data points using monoexponential decay function.
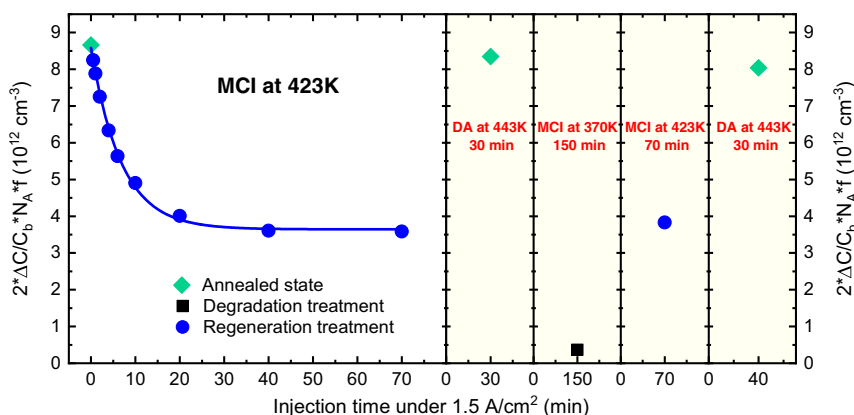
Figure 2. Changes in the concentration of the B_sO_2 donor state upon a regeneration-like treatment at 423 K with $J_{FB} = 1.5\,\mathrm{A\,cm^{-2}}$ (left) in a 10 Ω cm boron-doped n^+–p diode. Changes in the concentration of the BO defect (colored filled) after different treatment following the first regeneration. The conditions of the treatment carried out are written in red. Measurements of the capacitance transients after the different treatments have been carried out at 350 K using Laplace DLTS technique.

same effect can be observed in Figure 1 for the diode from 3 Ω cm material. However, in this material the degradation rate, which is proportional to squared hole concentration,[1,2] is significantly faster than the annealing rate, so nearly all the B_sO_2 defects are transformed to the degraded state after a long treatment.

After the first regeneration treatment, it can be observed that the dark annealing results in the total recovery of the B_sO_2 donor state concentration in agreement with the results presented in Figure 1. To convert the annealed state into the degraded state, a one-step degradation treatment (forward-bias-induced minority carrier injection at 370 K for 150 min) has been carried out which results in the complete disappearance of the B_sO_2 defect deep donor state. At 370 K, the annealing rate is very slow and thus the degradation reaction results in the complete disappearance of the donor state of the B_sO_2 defect.

Subsequently, the one-step regeneration treatment has been applied to the diode with the B_sO_2 defect in the degraded state (to compare its result with that of the treatment which started with the B_sO_2 defect in the annealed state in the previous experiment). This treatment resulted in the partial recovery of the B_sO_2 defect donor state to the saturation value which is close to that obtained after the first detailed regeneration treatment. The stability of the obtained decrease in the concentration of the B_sO_2 defect donor state (relative to the initial concentration) has been examined via dark annealing at 443 K. Again, the total recovery of the B_sO_2 defect concentration has been achieved after the annealing treatment.

Overall, the total recovery of the concentration of the deep donor state of the BO defect by annealing means that the degradation will occur again upon minority carrier injection at room temperature. It can be concluded that what has been referred to as "regeneration" in the experiments described above and presented in Figure 1 and 2 by the blue squares is not an actual regeneration reaction, but rather a degradation reaction with partial recovery due to the annealing reaction. The initial state of the BO defect, to which the regeneration treatment is applied (annealed state or degraded state), has no effect on the resultant state after the regeneration-like treatments (Figure 2). Importantly, we have not obtained any evidence of the permanent disappearance of the B_sO_2 defect upon regeneration-like treatments in the Cz-Si:B samples, which contain negligible concentrations of hydrogen.

2.2. Interaction of Hydrogen Atoms with Boron–Dioxygen Complexes

2.2.1. Hydrogen Introduced via Wet Chemical Etching

To investigate the interaction between hydrogen atoms and the B_sO_2 defect, Schottky barrier diodes (SBDs) have been fabricated on the boron-doped Cz-Si materials. For this presentation, we have chosen a material with high initial concentration of the B_sO_2 defect for the sake of clear monitoring of any changes in the defect concentration after treatments. It is well known that the chemical treatments of p-type Si materials we have used introduce some hydrogen, which passivates electrical activity of shallow acceptor impurities in the subsurface region of samples.[23] Particularly, we have carried out wet chemical etching of some samples intentionally to increase the concentration of hydrogen, which is positively charged in p-type materials, in the subsurface regions. We have monitored the changes in the concentration of ionized uncompensated boron atoms by an analysis of $N_A^-(W)$ dependencies obtained from the capacitance–voltage (C–V) measurements as shown in **Figure 3**a. The strong drop in the concentration of uncompensated ionized boron atoms close to the surface in the initial profile (black line in Figure 3a) is due to the interaction of H^+ with B_s^-, thus forming neutral BH complexes.[23] The $N_A^-(W)$ values for depth $> 1.1\,\mu m$, i.e., in the deeper bulk region, are nearly constant at about $1.1 \times 10^{16}\,\mathrm{cm^{-3}}$.

We have used C–V measurements to choose the reverse bias and the filling pulse voltages to be used in conventional DLTS measurements in order to probe the bulk region which is hydrogen-free initially. The resultant DLTS spectrum in the
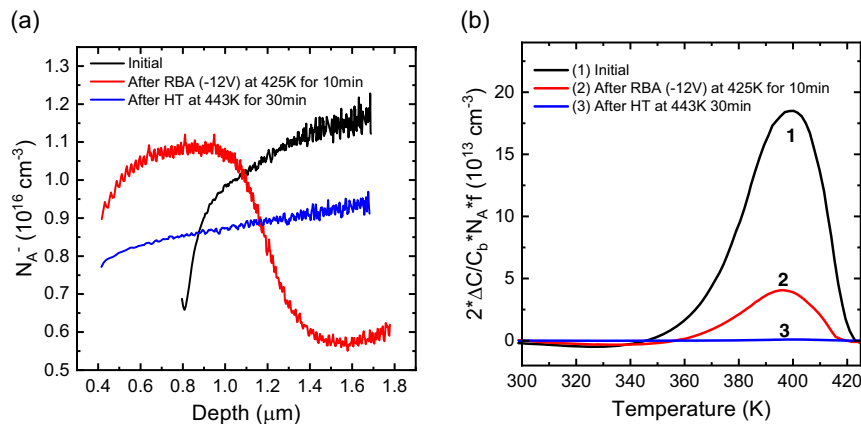
Figure 3. a) Depth profiles of the ionized uncompensated dopant concentration, $N_A^-(W)$, in a boron-doped Cz-Si sample, which was hydrogenated via wet chemical etching (initial) and subjected to RBA at 425 K and a heat treatment (HT) at 443 K without bias applied. The profiles have been calculated from the C–V dependences measured at 320 K. b) Conventional DLTS spectra recorded in the temperature range 300–425 K with rate window $R = 10\,\mathrm{s}^{-1}$ and filling pulse width $t_p = 200\,\mathrm{ms}$ on the same sample before and after the aforementioned treatments. The bias and pulse voltages have been selected according to C–V measurements to probe the same region between 1.1 and 1.45 μm from the surface in the three cases.

temperature range 300–425 K on the initial (as-processed) diode is presented in Figure 3b as the black line (spectrum 1). We have detected a hole emission signal with its maximum at about 390 K related to the deep donor state of the B_sO_2 defect with relatively high concentration of about $2 \times 10^{14}\,\mathrm{cm}^{-3}$.

Subsequently, the diode was kept at 425 K with the applied reverse bias of 12 V for 10 min. This treatment, referred to as RBA treatment, provides the thermal energy needed to release hydrogen from the B_s–H complexes close to the surface and promote the electric field-induced drift of positively charged hydrogen atoms into the bulk region. It can be observed in Figure 3a that the RBA treatment caused significant changes in the $N_A^-(W)$ profile. The concentration of the uncompensated ionized shallow acceptor atoms is increased in the subsurface region but is decreased deeper in the bulk region. This indicates that positively charged hydrogen atoms were moved into the bulk region where they interact with the negatively charged boron atoms. To monitor the changes in the concentration of the B_sO_2 defect after the RBA treatment, we have recorded another conventional DLTS spectrum in the temperature range 300–425 K in the same depth region, which was probed in the DLTS measurements before the RBA treatment (Figure 3b). A significant drop in the concentration of the deep donor state of the B_sO_2 defect from $\approx 1.8 \times 10^{14}$ to $\approx 4 \times 10^{13}\,\mathrm{cm}^{-3}$ has been induced by the RBA treatment. To examine the stability of the RBA-induced effect, we have carried out annealing of the sample at 443 K for 30 min without bias. This annealing treatment is known to result in the recovery of the annealed state of the B_sO_2 defect after LID. The $N_A^-(W)$ profile, shown in Figure 3a, indicates that the hydrogen content has been redistributed during the annealing treatment between the subsurface region and the bulk region that resulted in an approximately constant uncompensated ionized shallow acceptor concentration of about $9 \times 10^{15}\,\mathrm{cm}^{-3}$ all over the depletion region. For the bulk region (depth $> 1.1\,\mu\mathrm{m}$), this value is less than the initial bulk N_A^- value before any treatments but higher than the value reached after RBA which means that hydrogen boron pairs are dissociated in the bulk region upon the annealing

treatment. For the subsurface region (depth $< 1.1\,\mu\mathrm{m}$), the N_A^- value after annealing is higher than the initial value but less than the value after RBA. So, a comparison of the $N_A^-(W)$ profiles in Figure 3a indicates that hydrogen diffused in all directions when annealing is performed without bias at 443 K. Importantly, no recovery of the DLTS signal was obtained after the annealing treatment, but we have observed a further reduction in the concentration of the deep donor state of the B_sO_2 defect to a very low concentration of $\approx 9.3 \times 10^{11}\,\mathrm{cm}^{-3}$ (Figure 3b). The reduction in the concentration of the B_sO_2 defect upon the heat treatment at 443 K is related to its passivation by hydrogen atoms released from the unstable B–H pairs at this temperature, that is consistent with the observed change in the $N_A^-(W)$ profiles in Figure 3a. This finding shows that the observed drop in the B_sO_2 defect concentration after RBA at 425 K is stable at a temperature of 443 K.

2.2.2. Hydrogen Introduced via Remote Plasma

To further investigate the effect of hydrogenation on the B_sO_2 defect concentration, we have carried out similar measurements on another set of SBDs fabricated on the same boron-doped material. The samples from this set were hydrogenated via remote radiofrequency (RF) hydrogen plasma prior the deposition of metals for fabrication of Schottky diodes. The hydrogen plasma treatment was carried out to introduce significant amounts of hydrogen exceeding those introduced via wet chemical etching. The initial (as-processed) concentration-depth profile of a H plasma-treated sample is shown in **Figure 4**a. It can be observed that the hydrogenation via the H plasma treatment introduced significant amounts of hydrogen into the subsurface region which results in the steep drop of concentration of N_A^- from $\approx 1.5 \times 10^{16}\,\mathrm{cm}^{-3}$ in the bulk region to nearly zero at $\approx 0.7\,\mu\mathrm{m}$ from the surface. The N_A^- drop in the subsurface region was less powerful in samples hydrogenated via wet chemical etching compared to that in the samples hydrogenated via H plasma as can be seen from a comparison of the $N_A^-(W)$ initial profiles in Figure 3a and 4a. This confirms that the treatment in
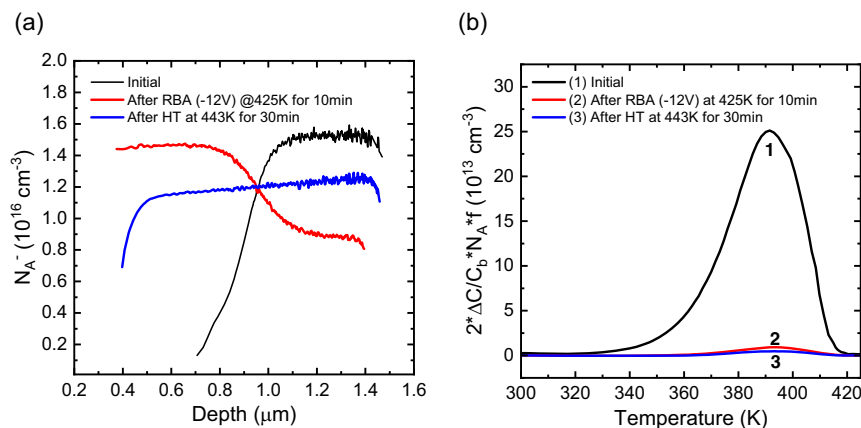
Figure 4. a) Depth profiles of the ionized uncompensated dopant concentration, $N_A^-(W)$, in $1\,\Omega\,cm$ boron-doped Cz-Si sample, which was hydrogenated via remote RF hydrogen plasma (initial) and subjected to RBA at 425 K and a HT at 443 K without bias applied. The profiles have been calculated from the $C-V$ dependences measured at 320 K. b) Conventional DLTS spectra recorded in the temperature range 300–425 K with rate window $R = 10\,s^{-1}$ and filling pulse width $t_p = 200\,ms$ on the same sample before and after the aforementioned treatments. The bias and pulse voltages have been selected according to $C-V$ measurements to probe the same region between 1.0 and 1.35 μm from the surface in the three cases.

remote hydrogen plasma introduces higher concentration of hydrogen into the subsurface region.

We have carried out the same experiments on the samples hydrogenated via the treatment in H plasma. Figure 4b shows the conventional DLTS spectra recorded in the temperature range 300–425 K on a H plasma hydrogenated diode before and after an RBA treatment at 425 K and annealing treatment at 443 K. A very sharp drop in the concentration of B_sO_2 defect occurs as a result of the RBA treatment as can be seen in Figure 4b. The RBA treatment induced the dissociation of the initially formed BH pairs in the subsurface region and the drift of positively charged hydrogen atoms into the bulk region (as monitored via $N_A^-(W)$ profiles in Figure 4a). Relative to the initial magnitude of the hole emission-related signal with its maximum at about 390 K in the DLTS spectra, the sample hydrogenated via H plasma has shown about 25 times smaller peak magnitude after the RBA treatment compared to about 4.5 times drop in the peak magnitude in the sample hydrogenated via wet chemical etching (Figure 3b vs Figure 4b). A further small drop in the concentration of the B_sO_2 defect has been observed after dark annealing at 443 K of the H plasma-hydrogenated sample, indicating that the RBA-induced decrease in the B_sO_2 defect concentration is thermally stable upon dark annealing at 443 K (Figure 4b).

We have carried out detailed Laplace DLTS measurements to obtain the spatial profiles of the B_sO_2 defect concentration in the H plasma-hydrogenated sample. **Figure 5** shows the concentration profiles of the B_sO_2 defect over the depletion region depth before and after an RBA treatment. It can be observed that the RBA treatment results in the decrease in the B_sO_2 defect concentration in all the studied regions compared to approximately uniform profile in the initial hydrogenated sample. However, the scale of the RBA-induced decrease in the B_sO_2 defect concentration is not uniform and at least three different regions can be identified: the deep bulk region at depth $> 1.2\,\mu m$, where the most significant drop in the B_sO_2 defect was obtained (nearly all the B_sO_2 defects have disappeared); the midregion between
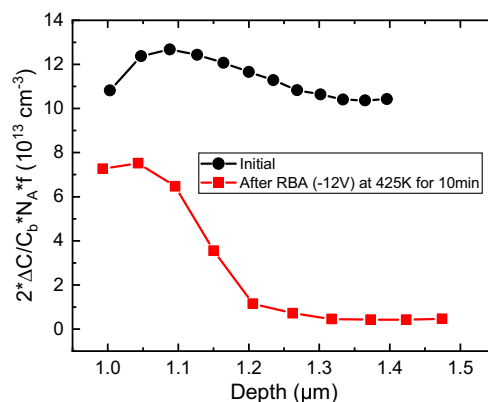

Figure 5. Depth profiles of B_sO_2 defect concentration in $1\,\Omega\,cm$ boron-doped Cz-Si:B material before (initial) and after RBA at 425 K for 10 min. Measurements of the capacitance transient have been carried out at 320 K using Laplace DLTS technique. Measurements have been carried out with variable bias and pulse voltages (U_b and U_p, respectively) with the difference of 2.0 V between U_b and U_p values.

$1.1 < depth < 1.2\,\mu m$, where the drop in the B_sO_2 defect concentration follows a negative slope straight line; and the subsurface region at depth $< 1.1\,\mu m$, where the least drop in the concentration of B_sO_2 was obtained.

The distribution of the B_sO_2 defects after the RBA treatment coincides inversely with the amount of hydrogen present in each of the three regions. The majority of hydrogen atoms have moved during the RBA treatment and are in the region with depth $> 1.2\,\mu m$ as can be noticed from an analysis of the $N_A^-(W)$ profiles in Figure 4a. Importantly, a high concentration of hydrogen is still available to interact with B_sO_2 defects even if BH pairs are formed. The concentration of ionized uncompensated boron atoms drops down to about $9 \times 10^{15}\,cm^{-3}$ after RBA (red $N_A^-(W)$ profile in Figure 4a), while it was close to zero when nearly all hydrogen atoms were involved in the formation of BH

pairs as can be seen in the initial $N_A^-(W)$ profile in the same figure. Thus, only a part of the available hydrogen was involved in the formation of BH pairs in the bulk region, while another part interacted with the B_sO_2 complexes. In the subsurface region, the concentration of hydrogen introduced via plasma was very high initially, but the majority of these hydrogen atoms were bound to boron in the form of BH pairs. This means that hydrogen was indeed not available for the interaction with B_sO_2 complexes in this region. During RBA treatment, hydrogen atoms were released from the BH pairs but the majority of H^+ species drifted in the electric field into the bulk region to a depth which depends on the applied reverse bias. This gives only small chance for the interaction of the free hydrogen atoms with the B_sO_2 defects in this region and, thus, the observed drop in the B_sO_2 defects concentration is minimal. In between these two regions, a transition in the concentration of hydrogen from a minimum value to a maximum value occurs. This is reflected by the inverse trend of the decrease in the concentration of the B_sO_2 defects from a maximum to a minimum value upon the application of RBA unlike the initial case where it was almost uniform.

2.3. Modeling of Hydrogen Interactions with the B_sO_2 Complexes

Previous work indicated that the most stable B_sO_2 complexes in Si comprise an interstitial oxygen dimer next to a substitutional boron atom, B_s, with no direct B—O bonds formed.[3,5,24] Importantly, B_sO_2 is bistable, while in p-type Si it is a deep donor (D-state), where the oxygen dimer adopts a "square" configuration; under reverse bias conditions (or under minority carrier injection) the defect converts to a shallow acceptor state (A-state) with the O_2 unit in a staggered configuration. Besides the A-form, at least two metastable shallow acceptor structures, named A′ and A″, with energy 0.23 and 0.38 eV above A were found. It has been suggested that the B_sO_2 complex in A′ form is responsible for the lifetime degradation.[3]

Our calculations indicate that the interactions between hydrogen and the B_sO_2 complex in D-state (deep donor) results either in complexes with marginal binding energies or in the breaking of the squared O_2 units, which ultimately convert to a staggered form after atomic relaxation. These results suggest that besides the hindering effect of Coulomb repulsion between $BO_2^+(D)$ and H^+, thermodynamics also works against the formation of $B_sO_2(D)$–H in p-type Si.

The attachment of H^+ to structures A, A′, and A″ of BO_2^- leads to the formation of stable B_sO_2–H complexes. The two lowest energy configurations are depicted in **Figure 6**a,b. The H atom (black sphere) sits close to the center of a Si—B bond, next to the negatively charged B atom (green sphere). The formation of such complexes could explain the regeneration of degraded cells as the relocation of hydrogen released from B–H pairs and subsequently trapping by $B_sO_2(A)$ and $B_sO_2(A′)$ complexes.

To find support for the above model, an important question to address is whether H can actually passivate the B_sO_2 complexes. Comparing the electron affinity of B_sO_2–H structures with the same quantity for a 512-atom pristine supercell, we have found that the $(-/0)$ transition level of B_sO_2–H resides above the conduction band minimum for both A and A′ configurations.
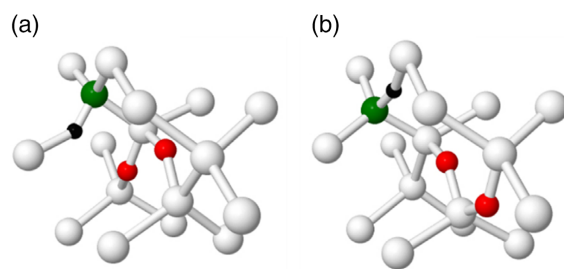

Figure 6. Atomistic models of the most stable structures of B_sO_2–H in Si. Silicon, boron, oxygen, and hydrogen are shown in white, green, red and black, respectively. a) Structure of $B_sO_2(A)$ passivated by H. b) Structure of $B_sO_2(A′)$ passivated by H.

Hence, as in the reaction between B and H,[25] the acceptor level of B_sO_2 is removed from the gap as a result of its connection to H. No donor transitions were found either.

While the calculations indicate that B_sO_2–H complexes are electrically inert, it is also important to know how stable these complexes are in comparison with boron–hydrogen pairs. More specifically, is the conversion of BH pairs into B_sO_2–H a reaction with a favorable energy balance?

Table 1 reports the energy balance (ΔE) of several defect reactions involving hydrogen, boron, and B_sO_2 complexes in silicon. Negative values of ΔE indicate favorable (exothermic) reactions. Reactions identified in the table as (1)–(3) were already studied in ref. [25]. They show that the binding energy of a bond-centered proton (ground state of hydrogen in p-type Si) to B_s^- is 0.73 eV. We also found, as reaction (2) shows, that boron can bind at least to two H atoms ($\Delta E = -0.40$ eV for the capture of the second proton), and that the exchange of H between BH pairs is not energetically favored ($\Delta E = 0.34$ eV). More importantly in the present context, reaction (4) and (5) show that the binding energy of H to B_sO_2 exceeds the analogous quantity of H to substitutional boron by about 0.1 eV (see reaction (6) and (7)).

2.4. Formation of A_sO_2–H Complexes in Al- and Ga-Doped Cz-Si Materials

It has been previously shown that the oxygen dimer interacts with any substitutional group III acceptor atoms in silicon

Table 1. Energetics of several reactions of interest involving hydrogen, boron, and BO_2 complexes in Si. Negative energies balances refer to exothermic reactions. Defects are referred using the usual notation—superscripted symbols refer the charge state, while HBC stands for bond-centered hydrogen.

Reaction	ΔE [eV]	Identifier
$B_s^- + H_{BC}^+ \rightarrow BH^0$	−0.73	(1)
$BH^0 + H_{BC}^+ \rightarrow BH_2^+$	−0.40	(2)
$2BH^0 \rightarrow B_s^- + BH_2^+$	+0.34	(3)
$BO_2^-(A) + H_{BC}^+ \rightarrow BO_2^0(A)$–H	−0.85	(4)
$BO_2^-(A′) + H_{BC}^+ \rightarrow BO_2^0(A′)$–H	−0.83	(5)
$BH^0 + BO_2^-(A) \rightarrow B_s^- + BO_2^0(A)$–H	−0.12	(6)
$BH^0 + BO_2^-(A′) \rightarrow B_s^- + BO_2^0(A′)$–H	−0.10	(7)

and forms A_sO_2 (A_s = B, Al, Ga, or In) complexes with very similar electronic properties.[5,26] All the A_sO_2 complexes are found to be defects with negative-U properties. The values of the $E(-/+)$ occupancy level, activation energy for hole emission from the donor state, energy barriers, and frequencies for transition between different configurations of the different A_sO_2 complexes have been determined and compared in refs. [5,26]. Evidence of the interactions between hydrogen and the complexes made of a substitutional acceptor atom and the oxygen dimer are obtained in this study by means of conventional DLTS measurements on hydrogenated silicon crystals doped with aluminum and gallium impurities.

We have processed the samples from Cz-Si wafers doped with either Ga or Al in a similar way as the wafers doped with boron were processed. Hydrogen was introduced into the Cz-Si:Ga and Cz-Si:Al samples via wet chemical etching. A similar hole emission-related signal with its maximum at about 390 K has been detected in the conventional DLTS spectra of the Ga- and Al-doped materials as shown in **Figure 7** and **8**.

Figure 7 shows the DLTS spectra recorded in the temperature range 300–425 K before and after RBA of a diode made on a hydrogenated Ga-doped Cz-Si sample. A decrease in the concentration of Ga_sO_2 complexes has been observed, but the decrease is much less significant than in the case of boron-doped samples. The $N_A^-(W)$ profiles (shown in the inset of Figure 7) indicate that large amounts of hydrogen atoms have moved into the bulk region after RBA and passivated Ga_s^- atoms in the bulk. A comparison of the ratios of passivated Ga_s^- and $Ga_sO_2^-$ defects to their initial values in the bulk regions suggests that the hydrogen interacts more efficiently with single gallium atoms than with the Ga_sO_2 complexes.

Figure 8 shows the changes in the concentration of the Al_sO_2 complexes in a hydrogenated Cz-Si:Al sample after RBA treatments at different temperatures. It can be seen that the RBA treatment at 420 K of the Al-doped Cz-Si sample results in a relatively small decrease in the concentration of Al_sO_2 complexes (see Figure 8). Only after RBA with the same reverse bias voltage
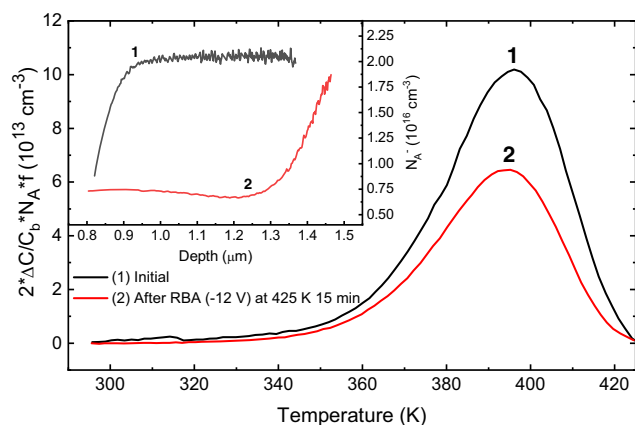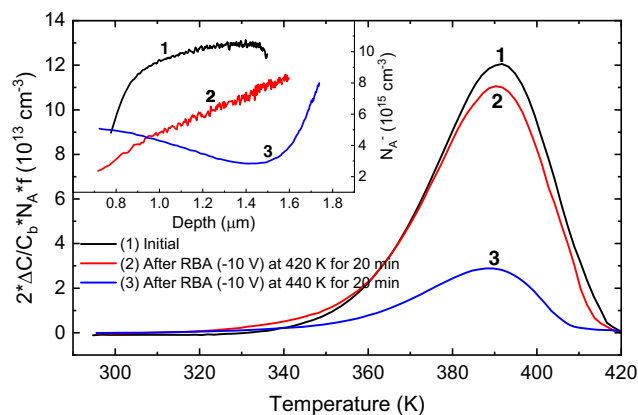

Figure 8. Conventional DLTS spectra recorded on hydrogenated Al-doped Cz-Si material before and after the RBA treatment in the temperature range 300–425 K with rate window $R = 10 \, s^{-1}$ and filling pulse width $t_p = 200$ ms. The depth profiles of the ionized uncompensated dopant concentration, $N_A^-(W)$ before and after the RBA treatments are shown in the inset.

(-10 V) at 440 K is applied, a significant drop in the concentration of Al_sO_2 complexes has been observed. The $N_A^-(W)$ profiles (shown in the inset of Figure 8) indicate that relatively small concentration of hydrogen moved into the bulk from sub-surface regions after RBA at 420 K. The concentration of hydrogen relocated into the bulk has increased significantly after RBA at 440 K and the concentration of the Al–H pairs near the surface has decreased. The results obtained show that the Al–H pairs are dissociated more effectively at 440 K, and hydrogen atoms, which have been moved into the bulk regions upon RBA, interact effectively with both Al_s^- and $Al_sO_2^-$ defects.

3. Discussion

Recently, the BO-LID has been linked with the structural transformation of the B_sO_2 complex, and the peak with its maximum at about 390 K detected in conventional DLTS spectra has been assigned to hole emission from the donor state of this complex.[3,4] The details of the electronic properties of the B_sO_2 defect and its transformations upon the injection of minority carriers have been reported.[3] The B_sO_2 complex in the donor state can be considered as a precursor of the recombination active BO-LID defect, and its concentration can be monitored by measurements of the strength of the emission signal with its maximum at about 390 K. Disappearance of this hole emission signal can be caused by either: 1) the degradation reaction, by which the B_sO_2 defect is converted from the deep donor (annealed state) into the shallow acceptor state (degraded state) upon minority carrier injection at room temperature or slightly above it; and 2) regeneration reaction, by which the B_sO_2 defect is converted into the regenerated state upon minority carrier injection at slightly elevated temperature (398–473 K). Subsequent annealing in dark at about 473 K for about 10 min can be used to evaluate which of these reactions have occurred. The recovery of the B_sO_2-related hole emission signal after dark annealing at 473 K shows that the degradation reaction occurred, while the

Figure 7. Conventional DLTS spectra recorded on hydrogenated Ga-doped Cz-Si material before and after the RBA treatment in the temperature range 300–425 K with rate window $R = 10 \, s^{-1}$ and filling pulse width $t_p = 200$ ms. The depth profiles of the ionized uncompensated dopant concentration, $N_A^-(W)$ before and after the RBA treatment are shown in the inset.

absence of the dark-annealing-induced recovery of the signal indicates that the regeneration reaction happened.

The total dark-annealing-induced recovery in the concentration of the donor state of the B_sO_2 defect in non-hydrogenated Cz-Si:B samples after the application of forward-bias-induced minority carrier injection at 423 K indicates that the MCI treatment has not initiated the regeneration reaction but rather the degradation reaction, which is faster in the material with lower resistivity (Figure 1 and 2).

It has been argued in a few studies that the BO-LID regeneration consists of two processes.[14,16] Hydrogen plays a key role in one of them, while the second one occurs without hydrogen.[14,16] Our results on the effects of regeneration-like treatments on the concentration of donor state of the B_sO_2 defect in n^+–p diodes show that no permanent deactivation of the B_sO_2 defect can happen in the non-hydrogenated samples. These findings are not consistent with the suggested non-hydrogen related regeneration mechanism of BO-LID,[14,16] and support the arguments that the presence of hydrogen in the bulk is crucial for occurrence of the regeneration process.[12,13]

The goals of the RBA treatments applied in our study to the hydrogenated B-doped Cz-Si samples were the following: 1) to transform the B_sO_2 defects into the shallow acceptor state; 2) to release H atoms from the B_s–H complexes which were formed upon hydrogenation; and 3) to initiate the interaction of H^+ atoms with the $B_sO_2^-$ defect. In the depleted regions of Schottky diodes created by the application of reverse bias, the Fermi level position is at midgap, so the B_sO_2 complex, having the $E(-/+)$ occupancy level at about $E_v + 0.31$ eV,[3–5] is in the negatively charged state, $B_sO_2^-$. Strong Coulombic force-induced attraction occurs between the positively charged hydrogen atoms H^+ and the negatively charged $B_sO_2^-$ complex if hydrogen is available. We have not observed any newly formed electrically active defects in the DLTS spectra recorded after the RBA treatments. Thus, RBA initiates the interaction of H^+ with the $B_sO_2^-$ complex and results in the formation of B_sO_2–H complexes that explains the significant drop in the concentration of deep donor state of the B_sO_2 defect or even complete passivation of the defect if more hydrogen is incorporated. Experimental and ab initio modeling results above clearly support a picture according to which regeneration involves the passivation of the B_sO_2 complexes (either precursor or recombination active forms A or A', respectively), via the reaction with H released from BH pairs upon heat, illumination, and/or injection treatments.

In the boron-doped material, the complete passivation of the B_sO_2 defect by hydrogen means, in the context of LID, that the BO defect precursor (annealed state of the BO-LID defect) is no longer available to be converted into the shallow acceptor state which is recombination active upon minority carrier injection (the regenerated state has been formed upon RBA).

Similar interactions occur between hydrogen and the Al_sO_2 and Ga_sO_2 complexes, but the observed passivation effects were only partial. It seems that even though hydrogen is available in the bulk, the hydrogen interactions with single acceptor atoms A_s (Ga_s and Al_s) are more efficient than the interactions with the A_sO_2 complexes. This can be attributed to different structural configurations of the Al_sO_2 and Ga_sO_2 complexes compared to those for B_sO_2,[5] which could lead to weaker binding energies

to H, and favor the interactions of hydrogen with single Al and Ga acceptor atoms unlike the case of boron.

If the concentration of hydrogen introduced into the bulk region is high, such as that introduced via hydrogen plasma compared to that introduced via wet chemical etching, the passivation effect of the B_sO_2 complex is more pronounced. We have observed nearly complete disappearance of the B_sO_2 related DLTS signal after RBA in the samples hydrogenated with remote H plasma. This is in agreement with the results reported in the literature about more powerful regeneration or accelerated passivation of the BO-LID defect when the concentration of hydrogen in the bulk regions is higher,[11,13,17,27] even though the method of hydrogen incorporation is different. A clear correlation exists between the presence of free hydrogen at a certain region in the sample and the decrease in the concentration of the B_sO_2 complex. Therefore, our results support the suggestion that hydrogen is directly involved in the regeneration mechanism of the BO-LID defect, which can be identified as the H-induced passivation of the B_sO_2 complexes via the formation of stable B_sO_2–H complexes.

The hydrogen atoms must be free for any interactions with the A_sO_2 complexes to occur. This means that the A_s–H pairs, which act as the source of hydrogen, should be separated. The binding energies of hydrogen to the acceptor atoms are different for different acceptor atoms,[28] and the temperature needed to overcome these energies varies between 420 and 440 K for B-, Ga-, and Al-doped Si. According to our annealing experiments, the electrically neutral B_sO_2–H complexes are stable at 443 K, whereas the BH pairs formed in the bulk after RBA treatments dissociate at this temperature. This corroborates the ab initio modeling results, which predict a higher binding energy of the B_sO_2–H complexes than the analogous quantity for the BH pairs. In contrast, the other A_sO_2–H complexes (with A_s being either Ga or Al) seem to have binding energies comparable to those for the respective A_s–H pairs. This can explain the less pronounced decrease in the concentration of A_sO_2 defects after the RBA treatments where the dissociation rates of the A_s–H pairs and A_sO_2–H complexes determines the effectiveness of the passivation of the A_sO_2 defects.

4. Conclusion

In this article, we have attempted to understand the details of hydrogen interactions with the A_sO_2 (A = B, Al, Ga) complexes in p-type Cz-Si materials and, importantly, to elucidate how the interaction between hydrogen atoms and the B_sO_2 defect suppresses its recombination activity by the formation of the regenerated state. The investigation of changes in the B_sO_2 defect concentration upon regeneration-like treatments in n^+–p hydrogen-free diodes has shown that regeneration is not possible without the presence of hydrogen in the active region in agreement with results from previous studies. We found that without hydrogen, the application of the regeneration treatment (injection of minority carriers at slightly elevated temperature) results in the transformation of the defect into the degraded state rather than the regenerated state which then is converted back to the unstable annealed state upon dark annealing for few minutes at 473 K.

With hydrogen introduced into the subsurface region by means of wet chemical etching or hydrogen plasma treatment at room temperature, DLTS measurements were carried out on hydrogenated samples made from Cz-Si:B material before and after RBA treatments. We have used RBA to transform the B_sO_2 defect into the degraded state (shallow acceptor state), to release the introduced hydrogen atoms bounded initially to the acceptor atoms in the sub-surface region, and to move the H atoms into the bulk region. The RBA treatments resulted in very significant drops in the concentration of the B_sO_2 defects. This has been attributed to the formation of electrically neutral B_sO_2–H complexes by the interaction of free positively charged hydrogen atoms H^+ and the negatively charged defects responsible for LID, $B_sO_2^-$. Upon dark annealing at 443 K, the formed B_sO_2–H complexes are stable unlike the BH pairs which dissociate at this temperature resulting in further passivation of the B_sO_2 defects by hydrogen. This is confirmed by ab initio calculations which show that the binding energy of H^+ to $B_sO_2^-$ exceeds that of H^+ to B_s^- by at least 0.1 eV.

The comparison between hydrogen introduction methods, i.e., wet chemical etching versus hydrogen plasma treatment, has revealed that the passivation of the B_sO_2 defects is more effective when more hydrogen is introduced into the bulk region. The investigation of spatial profiles of the B_sO_2 defects has shown a clear correlation between the presence of hydrogen at a certain region and the passivation effect where complete passivation of the $B_sO_2^-$ defects has been achieved in the region which contains the maximum concentration of hydrogen atoms.

Evidence of similar interactions between hydrogen and other acceptor–dioxygen complexes has been obtained from DLTS spectra recorded on samples from Cz-Si:Ga and Cz-Si:Al materials. However, the observed hydrogen-induced passivation of the Al_sO_2 and Ga_sO_2 defects is not as effective as for the Cz-Si:B case. A possible explanation of the different behavior after RBA treatments is that the B_sO_2–H complexes are more stable than BH pairs whereas other A_sO_2–H complexes have binding energies close to that of A_s–H pairs. Further ab initio calculations and experiments are needed to elucidate the difference in the interactions of hydrogen with different acceptor atoms and acceptor–dioxygen complexes.

5. Experimental Section

N^+–p and SBDs have been used to study the interactions of hydrogen atoms with A_sO_2 defects in Czochralski-grown silicon materials doped with either boron, aluminum, or gallium.

The n^+ region of the n^+–p diodes was formed by in-diffusion of phosphorous atoms from PCl_3 gas at high temperature into 3 and $10\,\Omega$ cm boron-doped Cz-Si wafers. The interstitial oxygen concentration $[O_i]$ in the 3 and $10\,\Omega$ cm diodes was about $(7.5 \pm 1) \times 10^{17}$ and $(9.5 \pm 1) \times 10^{17}\,cm^{-3}$, respectively, as estimated from measurements of the capture rate of interstitial carbon atoms by the O_i atoms in the diodes, which were irradiated with alpha particles at 260 K.[29,30] Some of the diodes were annealed at 400 °C for 10–15 h to increase the concentration of the BO defect. It is found that the concentration of hydrogen introduced into the base regions of the n^+–p diodes during fabrication is negligible.

For SBDs, plasma sputtering was used to deposit titanium/aluminum stack via a shadow mask on samples from p-type Cz-Si doped with either B, Al, or Ga, and gold was deposited via thermal evaporation on the back surface to act as an Ohmic contact. Samples were cleaned with trichloroethylene, acetone, and methanol and subjected to 1 min dipping in diluted (10%) HF before deposition of the metals. The diode area was 0.79 mm^2 with a leakage current of the order of $\approx 10^{-7}$ A at 16 V reverse bias voltage.

Hydrogen was introduced into the samples before fabrication of the Schottky diodes either via wet chemical etching in a mixture of $HF:HNO_3$ (1:7) or via treatments in remote RF hydrogen plasma at room temperature for 60 min. The H plasma treatments were carried out with 50 W RF power, 1–2 mbar chamber pressure, and 200–250 cc min^{-1} hydrogen gas flow.

Current–voltage (I–V) and capacitance–voltage (C–V) measurements were carried out to assess the quality of the diodes and determine the concentrations of uncompensated shallow acceptor atoms, the depth of the depletion region, and the bias voltage and pulse voltage used to probe the bulk and subsurface regions in electrical measurements. Conventional DLTS and high-resolution Laplace DLTS techniques were used to detect and characterize deep-level traps in the diodes.[31] Measurements were carried out before and after RBA treatments in the temperature range 398–448 K as well as after dark annealing at 443 K which was done in the furnace. The effect of these treatments on the concentration profiles of uncompensated shallow acceptor atoms has been monitored using C–V measurements while junction spectroscopy techniques have been used to monitor the changes in the concentration of deep-level defects.

The interactions of hydrogen with BO_2 complexes in silicon were further investigated using density functional theory within the projector-augmented wave/plane wave formalism[32] as implemented by the Vienna Ab initio Simulation Package (VASP).[33,34] Total energies were obtained using the electronic exchange–correlation functional of Heyd, Scuseria, and Ernzerhof (often referred to as HSE06),[35] which mixes a portion of exact Fock exchange for short-ranged interactions. This leads to a calculated bandgap of $E_g = 1.1$ eV, thus avoiding the severe underestimation of this quantity when using cheaper local and semilocal functionals.

The valence states were described by plane waves with a cutoff energy $E_{cut} = 400$ eV. Boron, oxygen, and hydrogen impurities were inserted in supercells with cubic shape and 512 Si atoms (with calculated lattice constant $a = 5.4318$ Å). For such large cells, we found that a Γ-point sampling of the Brillouin zone resulted in sufficiently accurate energy differences, including forces. The latter were evaluated within the generalized gradient approximation (GGA) to the exchange correlation potential,[36] from which minimum energy structures were found with a maximum residual force of 0.01 eV Å^{-1}. Total energies of defects with nonzero charge included a periodic charge correction.[37]

Conflict of Interest

The authors declare no conflict of interest.

Data Availability Statement

The data that support the findings of this study are available from the corresponding author upon reasonable request.

www.pss-a.com

[1] J. Schmidt, K. Bothe, *Phys. Rev. B* **2004**, *69*, 024107.
[2] T. Niewelt, J. Schön, W. Warta, S. W. Glunz, M. C. Schubert, *IEEE J. Photovoltaics* **2017**, *7*, 383.
[3] M. Vaqueiro-Contreras, V. P. Markevich, J. Coutinho, P. Santos, I. F. Crowe, M. P. Halsall, I. Hawkins, S. B. Lastovskii, L. I. Murin, A. R. Peaker, *J. Appl. Phys.* **2019**, *125*, 185704.
[4] V. P. Markevich, M. Vaqueiro-Contreras, J. T. De Guzman, J. Coutinho, P. Santos, I. F. Crowe, M. P. Halsall, I. Hawkins, S. B. Lastovskii, L. I. Murin, A. R. Peaker, *Phys. Status Solidi A* **2019**, *216*, 1900315.
[5] J. A. T. De Guzman, V. P. Markevich, I. D. Hawkins, J. Coutinho, H. M. Ayedh, J. Binns, N. V. Abrosimov, S. B. Lastovskii, I. F. Crowe, M. P. Halsall, A. R. Peaker, *J. Appl. Phys.* **2021**, *130*, 254703.
[6] A. Herguth, G. Schubert, M. Kaes, G. Hahn, *Prog. Photovolt. Res. Appl.* **2008**, *16*, 135.
[7] A. Herguth, G. Hahn, *J. Appl. Phys.* **2010**, *108*, 114509.
[8] V. Voronkov, R. Falster, *Phys. Status Solidi B* **2016**, *13*, 712.
[9] K. Münzer, in *Proc. 24th Eur. Photovolt. Sol. Energy Conf. Exhib.* WIP, Munich, Germany, **2009**, pp. 1558–1561.
[10] S. Wilking, A. Herguth, G. Hahn, *J. Appl. Phys.* **2013**, *113*, 194503.
[11] S. Wilking, S. Ebert, A. Herguth, G. Hahn, *J. Appl. Phys.* **2013**, *114*, 194512.
[12] N. Nampalli, B. Hallam, C. Chan, M. Abbott, S. Wenham, in *Proc. 42nd IEEE Photovolt. Spec. Conf.* IEEE, New Orleans, LA, **2015**, pp. 1–3.
[13] S. Wilking, J. Engelhardt, S. Ebert, C. Beckh, A. Herguth, G. Hahn, in *Proc. 29th Eur. Photovolt. Sol. Energy Conf. Exhib.* WIP, Munich, Germany, **2014**, pp. 366–372.
[14] D. C. Walter, J. Schmidt, *Sol. Energy Mater. Sol. Cells* **2016**, *158*, 91.
[15] B. Lim, K. Bothe, J. Schmidt, *J. Appl. Phys.* **2010**, *107*, 123707.
[16] L. Helmich, D. C. Walter, R. Falster, V. V. Voronkov, J. Schmidt, *Sol. Energy Mater. Sol. Cells* **2021**, *232*, 111340.
[17] S. Wilking, C. Beckh, S. Ebert, A. Herguth, G. Hahn, *Sol. Energy Mater. Sol. Cells* **2014**, *131*, 2.
[18] B. Hallam, M. Abbott, N. Nampalli, P. Hamer, S. Wenham, *J. Appl. Phys.* **2016**, *119*, 065701.
[19] P. Hamer, B. Hallam, M. Abbott, C. Chan, N. Nampalli, S. Wenham, *Sol. Energy Mater. Sol. Cells* **2016**, *145*, 440.
[20] B. Lim, K. Bothe, J. Schmidt, *Phys. Status Solidi RRL* **2008**, *2*, 93.
[21] A. Herguth, G. Schubert, M. Kaes, G. Hahn, in *Proc. 4th IEEE World Conf. Photovolt. Energy Convers.* IEEE, Waikoloa, HI, **2006**, pp. 940–943.
[22] S. Wilking, M. Forster, A. Herguth, G. Hahn, *Sol. Energy Mater. Sol. Cells* **2015**, *142*, 87.
[23] A. R. Peaker, V. P. Markevich, L. Dobaczewski, *Defects in Microelectronics Materials and Devices* (Eds: D. M. Fleetwood, S. T. Pantelides, R. D. Schrimpf), CRC Press, Boca Raton, USA **2008**, p. 27.
[24] M.-H. Du, H. M. Branz, R. S. Crandall, S. B. Zhang, *Phys. Rev. Lett.* **2006**, *97*, 256602.
[25] J. A. T. De Guzman, V. P. Markevich, J. Coutinho, N. V. Abrosimov, M. P. Halsall, A. R. Peaker, *Sol. RRL* **2021**, 2100459.
[26] J. A. T. De Guzman, V. P. Markevich, S. Hammersley, I. D. Hawkins, I. Crowe, N. V. Abrosimov, R. Falster, J. Binns, P. Altermatt, M. P. Halsall, A. R. Peaker, in *Proc. 47th IEEE Photovolt. Spec. Conf.* IEEE, Calgary, AB, **2020**, pp. 1013–1018.
[27] G. Krugel, W. Wolke, J. Geilker, S. Rein, R. Preu, *Energy Procedia* **2011**, *8*, 47.
[28] T. Zundel, J. Weber, *Phys. Rev. B* **1989**, *39*, 13549.
[29] V. P. Markevich, L. I. Murin, *Sov. Phys. Semicond.* **1988**, *22*, 574.
[30] L. F. Makarenko, M. Moll, F. P. Korshunov, S. B. Lastovski, *J. Appl. Phys.* **2007**, *101*, 113537.
[31] A. R. Peaker, V. P. Markevich, J. Coutinho, *J. Appl. Phys.* **2018**, *123*, 161559.
[32] P. E. Blochl, *Phys. Rev. B* **1994**, *50*, 17953.
[33] G. Kresse, J. Furthmuller, *Phys. Rev. B* **1996**, *54*, 11169.
[34] G. Kresse, J. Furthmüller, *Comput. Mater. Sci.* **1996**, *6*, 15.
[35] J. Heyd, G. E. Scuseria, M. Ernzerhof, *J. Chem. Phys.* **2003**, *118*, 8207.
[36] J. P. Perdew, K. Burke, M. Ernzerhof, *Phys. Rev. Lett.* **1996**, *77*, 3865.
[37] C. Freysoldt, J. Neugebauer, C. G. Van de Walle, *Phys. Rev. Lett.* **2009**, *102*, 016402.